CO Oxidation

DOI: 10.1002/ange.201100190

Supported Rhodium Oxide Nanoparticles as Highly Active CO Oxidation Catalysts**

*D. A. J. Michel Ligthart, Rutger A. van Santen, and Emiel J. M. Hensen**

Catalytic oxidation of carbon monoxide has been extensively studied because of its importance for CO removal from effluent streams, in particular from car exhaust.[1,2] Another more recent application is CO removal from hydrogen for use in polymer electrolyte membrane (PEM) fuel cells.[3,4] Owing to their high activity, noble metals such as Pt, Pd, Ru, Rh, and Au have been the subject of many studies.[5–13] Until recently, the dominant belief was that CO oxidation takes place on metal surfaces,[14–16] because CO binds much more strongly to metals than to metal oxides. Single-crystal studies have shown that oxidation of the metal surface leads to catalyst deactivation.[14,15,17] Recent studies employing in situ spectroscopic techniques, however, have found indications that the active surface of Pt,[18–20] Pd,[21] and Ru[22,23] may be oxidic in nature under conditions of CO oxidation. Somorjai and co-workers reported that the active phase in polymer-stabilized Rh nanoparticles for CO oxidation is a thin surface oxide, formation of which is dependent on the particle size.[24] The turnover frequency (TOF) increased fivefold with a decrease of the particle size from 7 to 2 nm. The particle-size effect was not observed after deposition of the Rh nanoparticles on ordered mesoporous silica (SBA-15).[25] The increased catalytic activity of a thin surface RhO_2 film on oxidation of a Rh single-crystal surface was also discussed recently.[26,27] Formation of Rh_2O_3, on the other hand, leads to deactivation.[28]

Herein we show that the TOF for CO oxidation at 110 °C of 1.3 nm Rh nanoparticles is two orders of magnitude higher than that of 7.2 nm nanoparticles when ceria is the support. In situ X-ray absorption spectroscopy evidences that the high activity of the very small nanoparticles is related to nearly complete oxidation of the initially reduced Rh nanoparticles. The tendency of Rh nanoparticles to become oxidized is size-dependent: Rh particles smaller than 2.5 nm are oxidized almost completely, whereas those larger than 4 nm remain metallic. Catalysts with Rh nanoparticles in the range of 1–9 nm were synthesized by variation of the Rh loading, the calcination temperature of the support and the catalyst, and optionally a high-temperature ageing treatment in H_2O/H_2. Because reducibility of the support is usually implicated in the stabilization of metal oxide particles, we included Rh nanoparticle catalysts based on ceria, ceria–zirconia, zirconia, and silica supports in our investigations. The presence of oxygen defects in the support leads to much higher activity of Rh/CeO_2 compared to Rh/ZrO_2. The support affects the dispersion of the metal oxide and thereby its CO oxidation activity.

For this work, we prepared Rh nanoparticles on several oxide supports by incipient wetness impregnation. The particle size d_{Rh} of the reduced catalysts was determined by high-resolution transmission electron microscopy and H_2 chemisorption. For example, variation of the Rh loading from 0.1 to 1.6 wt% on a CeO_2 support prepared by homogeneous precipitation of Ce^{3+} following urea decomposition[29,30] and subsequent calcination at 550 °C gave nanoparticles in the range of 1.3–2.8 nm. A catalyst containing 1.6 wt% Rh on the same ceria support calcined at 900 °C gave an average particle size of 5.2 nm. Larger particles with an average size of 7.2 nm were obtained by a reductive steaming treatment at high temperature.[31] Figure 1 shows TEM images of various ceria-supported catalysts. Below a particle size of about 3 nm it was difficult to image enough particles to obtain good statistics. In such cases, we resorted to H_2 chemisorption at −80 °C. We carefully checked that the particle sizes for a number of catalysts determined by using these two methods were similar. Rhodium nanoparticle catalysts supported by $CeZrO_2$, ZrO_2, and SiO_2 were prepared in a similar manner.

A suite of 30 samples were then tested for catalytic oxidation of CO in a parallel microflow reactor setup monitored by a gas chromatograph. Measurements were carried out in a mixture of 1 vol% CO and 1 vol% O_2 balanced by He under differential conditions in the temperature range 60-180 °C. Figure 2a shows the TOFs of these catalysts as a function of the particle size at a reaction temperature of 110 °C. The TOF was determined on the basis of the dispersion of the catalysts reduced at 450 °C. The trends are very similar at 60 and 140 °C (see Supporting Information). The TOF for ceria-supported Rh particles smaller than 2.5 nm was two orders of magnitude higher than particles of about 7 nm. There is a clear transition regime of catalysts containing particles between 2.5 and 4 nm. The activity of large Rh nanoparticles supported on ZrO_2 and SiO_2 was equally low, that is, there is no strong support effect on the catalytic activity in CO oxidation. In contrast, the TOF of Rh nanoparticles below 2.5 nm critically depends on the type of

[*] D. A. J. M. Ligthart, Prof. Dr. R. A. van Santen, Prof. Dr. E. J. M. Hensen
Schuit Institute of Catalysis, Eindhoven University of Technology
P.O. Box 513, Eindhoven (The Netherlands)
Fax: (+31) 40-245-5054
E-mail: e.j.m.hensen@tue.nl
Homepage: http://www.catalysis.nl

[**] The Soft Matter Cryo-TEM Research Unit at Eindhoven University of Technology and DUBBLE and its staff from the Netherlands Organization for Scientific Research (NWO) are acknowledged for access to the TEM and ESRF facilities, respectively. DAJML thanks Dr. Yejun Guan for valuable discussions.

Supporting information for this article is available on the WWW under http://dx.doi.org/10.1002/anie.201100190.

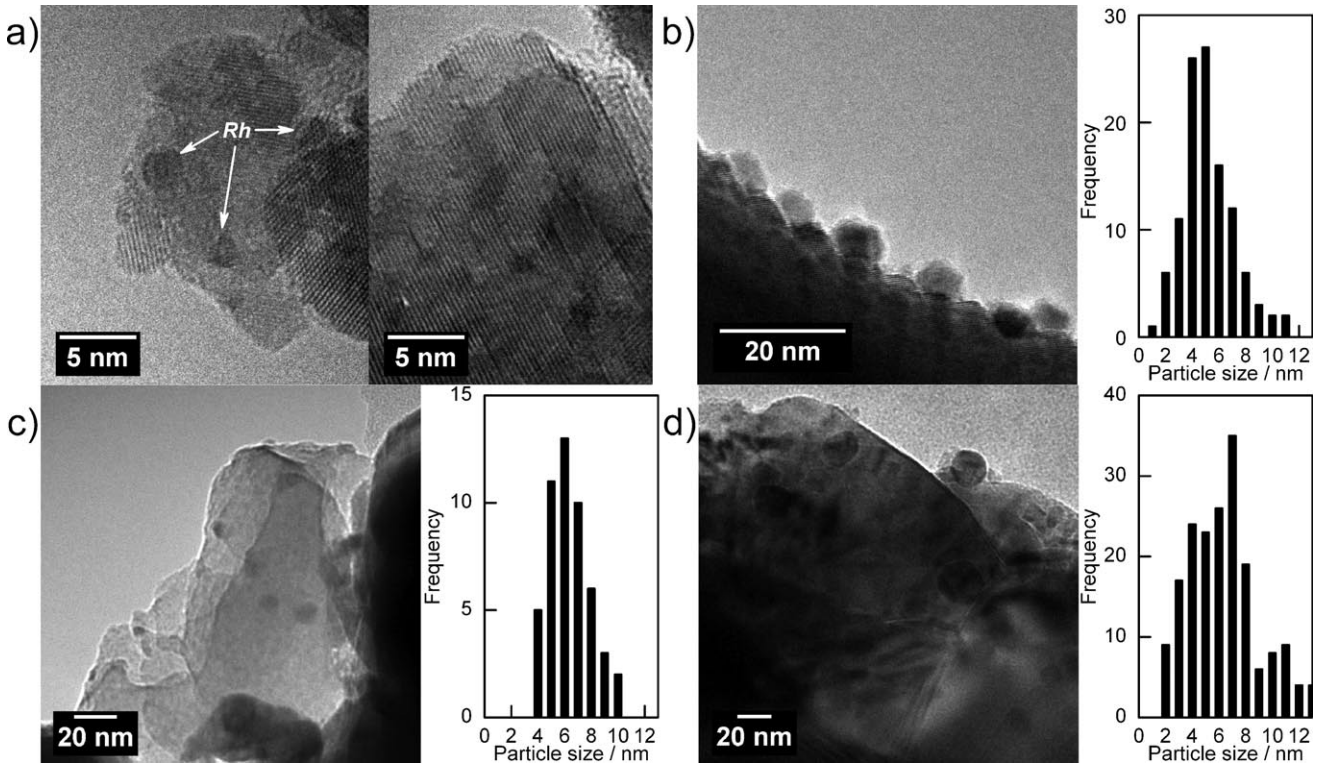

Figure 1. TEM images and Rh particle size distributions of a) Rh(2.8 nm)/CeO_2, b) Rh(5.2 nm)/CeO_2, c) Rh(6.3 nm)/CeO_2, and d) Rh(7.2 nm)/CeO_2. Due to the low contrast in TEM, the average particle size of Rh(2.8 nm)/CeO_2 was determined by H_2 chemisorption at −80 °C.

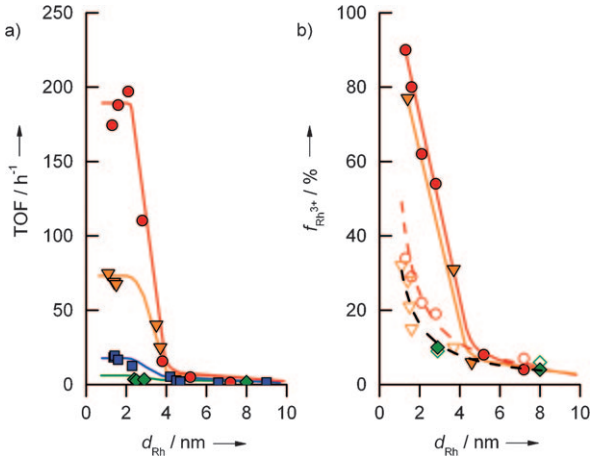

Figure 2. a) Turnover frequency in CO oxidation (T = 110 °C) and b) fraction of oxidic Rh $f_{Rh^{3+}}$ of supported Rh catalysts determined by XANES analysis as a function of the initial particle size d_{Rh} of the reduced catalysts (red circles: Rh/CeO_2; orange triangles: Rh/$CeZrO_2$; blue squares: Rh/ZrO_2; green diamonds: Rh/SiO_2; open symbols/dashed line: after reduction; closed symbols/full line: during CO oxidation).

support: the activity strongly increases in the order Rh/SiO_2 < Rh/ZrO_2 < Rh/$CeZrO_2$ < Rh/CeO_2.

In situ X-ray absorption spectroscopic measurements were carried out at the ESRF Dubble beamline.[32] An in situ cell connected to a gas-delivery system was employed in fluorescence mode at the Rh K-edge. The experimental procedure involved reduction of the catalyst in H_2 at 500 °C followed by recording a near-edge spectrum. The catalyst was then exposed to the same gas mixture as used in catalytic CO oxidation at 110 °C and a further near-edge spectrum was recorded. Figure 2b shows the oxidation degree $f_{Rh^{3+}}$ obtained by analysis of the near-edge spectra for Rh/CeO_2, Rh/$CeZrO_2$, and Rh/SiO_2 after reduction and during CO oxidation. Clearly, very small particles are not completely reduced during the H_2 treatment step at 500 °C, and Rh/CeO_2 is more difficult to reduce than Rh/$CeZrO_2$. Catalysts containing particles larger than about 4 nm are nearly completely reduced. Similar trends were observed for the other catalysts, except for Rh/SiO_2 (see Supporting Information). Under conditions of CO oxidation, significant changes in the near-edge spectra were observed for catalysts containing particles smaller than 2.5 nm with the exception of the silica-supported catalysts. It was not possible to obtain reliable data for Rh/ZrO_2 because of the overlap of fluorescence peaks of Rh and Zr. The nanoparticles supported on CeO_2 and $CeZrO_2$ became nearly fully oxidized. For instance, the oxidation degrees of Rh(1.3 nm)/CeO_2 during CO oxidation are 90 and 100 % at 110 and 140 °C, respectively. The oxidation degrees of Rh(1.4 nm)/$CeZrO_2$ are slightly lower under similar conditions. Conversely, particles larger than 4 nm remained metallic under CO oxidation conditions ($f_{Rh^{3+}}$ < 5 %). There is a strong correlation between the catalytic activity for CO oxidation and oxidation of the active phase. Nevertheless, by comparison of Rh nanoparticles smaller than 2.5 nm on CeO_2 and $CeZrO_2$ it follows that,

despite a similar degree of oxidation, the former catalyst is much more active than the latter.

The structure of two Rh/CeO_2 catalysts was analyzed by extended X-ray absorption fine structure (EXAFS) as a function of the gas atmosphere (H_2 at 500 °C, CO at 30 °C, O_2 at 110 °C, and $CO + O_2$ at 110 °C). The fit parameters are collected in Table 1 (for $\chi(k)\cdot k^3$ functions and Fourier transforms, see Supporting Information). The reduced Rh(2.1 nm)/CeO_2 catalyst contains an Rh–Rh shell. The small Rh–O contribution indicates that the Rh particles have not been completely reduced, in agreement with the near-edge analysis. Exposure to CO at room temperature results in a small decrease of the Rh–Rh coordination number, likely due to formation of Rh carbonyl complexes.[33] Exposure to O_2 at 110 °C leads to extensive oxidation of the 2.1 nm Rh nanoparticles, as follows from the increase of the Rh–O shell and the decrease of the Rh–Rh shell. Comparable results were obtained when the catalyst was exposed to CO oxidation conditions. These results are in contrast with the absence of changes to the structure and oxidation state of 7.2 nm Rh nanoparticles supported on ceria.

Table 1: Fraction of oxidic Rh $f_{Rh^{3+}}$ and fit parameters of k^3-weighted EXAFS spectra[a] at the Rh K-edge of Rh/CeO_2 catalysts containing 2.1 and 7.2 nm Rh particles on exposure to different gas conditions.

Treatment	$f_{Rh^{3+}}$ [%]	Shell[b]	N	R [Å]	$\Delta\sigma^2$ [Å^2]	E_0 [eV]
Rh(2.1 nm)/CeO_2						
H_2, 500 °C	24	Rh–O	0.5	2.03	0.003	5.2
		Rh–Rh	5.7	2.68	0.007	
CO, 30 °C	22	Rh–O	0.5	2.02	0.002	2.5
		Rh–Rh	4.4	2.69	0.006	
O_2, 110 °C	61	Rh–O	2.8	2.02	0.005	6.4
		Rh–Rh	3.7	2.68	0.008	
$CO + O_2$, 110 °C	59	Rh–O	2.3	2.03	0.004	1.5
		Rh–Rh	4.1	2.69	0.007	
Rh(7.2 nm)/CeO_2						
H_2, 500 °C	4	Rh–Rh	11.6	2.69	0.005	2.7
CO, 30 °C	1	Rh–Rh	10.9	2.69	0.005	1.0
O_2, 110 °C	1	Rh–Rh	11.0	2.69	0.006	2.7
$CO + O_2$, 110 °C	1	Rh–Rh	10.6	2.69	0.006	1.7

[a] Coordination number $N \pm 20\%$, coordination distance $R \pm 0.02$ Å, Debye–Waller factor $\Delta\sigma^2 \pm 10\%$, inner potential E_0. [b] Only first Rh–O and Rh–Rh shell reported.

The very high CO oxidation activity of very small Rh particles is related to their oxidation to small Rh oxide particles. Rh particles larger than 4 nm, which remain metallic, exhibit substantially lower activity. These activity differences go together with strong differences in the kinetic parameters of CO oxidation (see Supporting Information). The apparent activation energy E_{act} for Rh nanoparticles smaller than 2.5 nm is (68 ± 3) kJ mol^{-1} irrespective of the support, with the exception of a considerably higher value for Rh/SiO_2 catalysts. It increases significantly when the particles become larger than 2.5 nm. The E_{act} value for large particles increases in the order $CeO_2 \approx CeZrO_2 < ZrO_2$. The differences in E_{act} between small and large particles are in qualitative agreement with the values for unsupported Rh particles reported by Somorjai and co-workers.[24] The reaction order in CO is close to zero for the highly active catalysts and becomes -1 for the large metal nanoparticles. In all cases the reaction order in oxygen is found to be close to unity. For large particles, the high values of E_{act} and the negative first-order and first-order dependence in CO and O_2, respectively, are consistent with early data for CO oxidation on Rh(100) and Rh(111) crystal surfaces.[34] The CO reaction order of -1 implies a high CO surface coverage under reaction conditions. The first-order dependence in O_2 is due to the rate-controlling nature of oxygen chemisorption on a single Rh site followed by fast dissociation.[35] Thus, the CO oxidation reaction occurs on metallic Rh nanoparticles when their size is larger than 4 nm. The different kinetics for the Rh particles smaller than 2.5 nm point to a change in the CO oxidation mechanism. The E_{act} value is lower by nearly 40 kJ mol^{-1}, and the reaction is zero and first-order in CO and O_2, respectively. The kinetic data suggest that CO will be adsorbed much more weakly to the surface than on large metallic particles. This difference is due to the oxidic nature of the small Rh nanoparticles. The higher catalytic activity of these rhodium oxide particles is due to the lower E_{act} value. An explanation is the lower barrier for the surface reaction $CO + O \rightarrow CO_2$ on Rh oxide as compared to the Rh metal surface, as predicted by Gong et al.[36] On the other hand, the lower apparent activation energy for Rh oxide nanoparticles can also be explained by the lower CO coverage compared to the fully CO covered Rh surface, which increases the apparent activation energy.

An important kinetic finding is that the apparent activation energies of highly active Rh/CeO_2, $Rh/CeZrO_2$, and Rh/ZrO_2 are very similar. Consequently, we suspected that the reason for the much higher activity of Rh/CeO_2 compared to $Rh/CeZrO_2$ is the higher dispersion of the active metal oxide phase on ceria under CO oxidation conditions. One expects a higher dispersion of the active Rh oxide phase to result in higher O/Rh ratios under reaction conditions. To quantify the amount of reducible oxygen species, CO temperature-programmed surface reaction (CO-TPSR) was carried out, similar to previous studies for ceria- and silica-supported Pt and Au catalysts.[37,38] Reducible oxygen species of the active phase and the support react to form CO_2. The oxygen of the active Rh phase was determined by quantifying the amount of CO_2 below 250 °C (Table 2).[38] The O/Rh ratio of Rh(1.6 nm)/CeO_2 is much higher than that of Rh(1.6 nm)/$CeZrO_2$ in the temperature range 40–150 °C. This difference is interpreted in

Table 2: O/Rh ratio of reduced supported catalysts under O_2 and $CO + O_2$ atmosphere as determined by CO-TPSR.

Catalyst	O_2 atmosphere[a]		$CO + O_2$ atmosphere[a]	
	40 °C	150 °C	40 °C	150 °C
Rh(1.6 nm)/CeO_2	3.4	n.d.[b]	3.4	4
Rh(7.2 nm)/CeO_2	0.11	0.14	n.d.	n.d.
Rh(1.6 nm)/$CeZrO_2$	n.d.	n.d.	1.0	1.9
Rh(2.9 nm)/SiO_2	0.6	0.9	0.20	0.19
Rh(8.0 nm)/SiO_2	0.15	0.14	n.d.	n.d.

[a] Treatment prior to CO-TPSR: 5 vol% O_2/He or 3 vol% CO + 3 vol% O_2 in He. [b] Not determined.

terms of a much higher dispersion of RhO_x on ceria than on ceria–zirconia. Large Rh particles in Rh(7.2 nm)/CeO_2 contain only very little oxygen on exposure to O_2 in this temperature range. Interestingly, we find that small Rh particles on silica can be oxidized to some extent, but they are reduced again under CO oxidation conditions. This suggests that the tendency of very small Rh particles to be oxidized in an oxygen atmosphere is an intrinsic property,[24] but that a reducible support is needed to stabilize these oxidic particles under conditions of catalytic CO oxidation.

Somorjai and co-workers reported that a thin surface oxide layer formed on small metallic Rh nanoparticles stabilized by polyvinylpyrrolidone are more active in CO oxidation than larger metallic Rh particles.[24] Such differences were found to be absent when these particles interacted with a silica support.[25] In applications, Rh particles are nearly always stabilized by reducible supports such as ceria. Our findings significantly show that in such case very small Rh metal particles are completely oxidized under CO oxidation conditions, whereas particles larger than 4 nm remain metallic. The importance of the stabilizing effect of the support is evident from the much larger activity difference of nearly two orders of magnitude between ceria-supported Rh oxide and Rh metal particles as compared to the unsupported case. The dispersion of the active Rh oxide phase and thus the catalytic activity critically depend on the nature of the support.

Experimental Section

Supported Rh catalysts were prepared by incipient wetness impregnation of a solution of $Rh(NO_3)_3{\cdot}n\,H_2O$ on CeO_2, $CeZrO_2$, ZrO_2, and SiO_2, followed by calcination and ageing at various temperatures.

In situ X-ray absorption spectroscopy was carried out in a home-built stainless steel cell equipped with carbon-foil windows at DUBBLE of the European Synchrotron Radiation Facility (Grenoble, France). The catalytic activity in CO oxidation was measured in a parallel ten-flow microreactor system. Analysis was done by on-line gas chromatograph (Porapak Q, MS 5A, thermal conductivity detector). The feed contained 1 vol% CO and 1 vol% O_2 in He. Catalysts were reduced in 20 vol% H_2 at 450°C. The activation energy was determined in the temperature range 60–180°C. Reaction orders of CO (O_2) were determined at a constant 1 vol% O_2 (CO) flow by varying the CO (O_2) concentration from 0.5 to 5 vol%.

Detailed procedures for H_2 chemisorption, TEM, XAS, and CO-TPSR are given in the Supporting Information.

Received: January 10, 2011
Revised: February 28, 2011
Published online: April 20, 2011

Keywords: heterogeneous catalysis · nanoparticles · oxidation · rhodium · supported catalysts

[1] G. Ertl, *Angew. Chem.* **2008**, *120*, 3578; *Angew. Chem. Int. Ed.* **2008**, *47*, 3524.
[2] M. Shelef, R. W. McCabe, *Catal. Today* **2000**, *62*, 35.
[3] W. D. Deng, M. Flytzani-Stephanopoulos, *Angew. Chem.* **2006**, *118*, 2343 – 2347; *Angew. Chem. Int. Ed.* **2006**, *45*, 2285 – 2289.
[4] X. Cheng, Z. Shi, N. Glass, L. Zhang, J. Zhang, D. Song, Z. S. Liu, H. Wang, J. Shen, *J. Power Sources* **2007**, *165*, 739 – 756.
[5] I. E. Beck, V. I. Bukhtiyarov, I. Y. Pakhurakov, V. I. Zaikovsky, V. V. Kriventsov, V. N. Parmon, *J. Catal.* **2009**, *268*, 60 – 67.
[6] A. M. Doyle, S. K. Shaikhutdinov, S. D. Jackson, H. J. Freund, *Angew. Chem.* **2003**, *115*, 5398 – 5401; *Angew. Chem. Int. Ed.* **2003**, *42*, 5240 – 5243.
[7] A. Binder, M. Seipenbusch, M. Muhler, G. Kasper, *J. Catal.* **2009**, *268*, 150 – 155.
[8] S. Colussi, A. Gayen, M. F. Camellone, M. Boaro, J. Llorca, S. Fabris, A. Trovarelli, *Angew. Chem.* **2009**, *121*, 8633 – 8636; *Angew. Chem. Int. Ed.* **2009**, *48*, 8481 – 8484.
[9] A. M. Karim, V. Prasad, G. Mpourmpakis, W. W. Lonergan, A. I. Frenkel, J. G. Chen, D. G. Vlachos, *J. Am. Chem. Soc.* **2009**, *131*, 12230 – 12239.
[10] P. Nolte, A. Stierle, N. Y. Jin-Phillipp, N. Kasper, T. U. Schulli, H. Dosch, *Science* **2008**, *321*, 1654 – 1657.
[11] S. M. McClure, M. J. Lundwall, D. W. Goodman, *Proc. Natl. Acad. Sci. USA* **2009**, *106*, 1 – 6.
[12] M. Haruta, *Nature* **2005**, *437*, 1098 – 1099.
[13] H. Falsig, B, Hvolbæk, I. S. Kristensen, T. Jiang, T. Bligaard, C. H. Christensen, J. K. Nørskov, *Angew. Chem.* **2008**, *120*, 4913 – 4917; *Angew. Chem. Int. Ed.* **2008**, *47*, 4835 – 4839.
[14] F. Gao, Y. Cai, K. K. Gath, Y. Wang, M. S. Chen, Q. L. Guo, D. W. Goodman, *J. Phys. Chem. C* **2009**, *113*, 191.
[15] J. I. Flege, P. Sutter, *Phys. Rev. B* **2008**, *78*, 153402.
[16] F. J. Gracia, L. Bollmann, E. E. Wolf, J. T. Miller, A. J. Kopf, *J. Catal.* **2003**, *220*, 382.
[17] S. M. McClure, D. W. Goodman, *Chem. Phys. Lett.* **2009**, *469*, 1 – 7.
[18] B. L. M. Hendriksen, J. W. M. Frenken, *Phys. Rev. Lett.* **2002**, *89*, 046101.
[19] M. D. Ackermann, T. M. Pedersen, B. L. M. Hendriksen, O. Robach, S. C. Bobaru, I. Popa, C. Quiros, H. Kim, B. Hammer, S. Ferrer, J. W. M. Frenken, *Phys. Rev. Lett.* **2005**, *95*, 255505.
[20] J. Singh, E. M. C. Alayon, M. Tromp, O. V. Safonova, P. Gratzel, M. Nachtegaal, R. Frahm, J. A. van Bokhoven, *Angew. Chem.* **2008**, *120*, 9400 – 9404.
[21] T. Schalow, B. Brandt, D. E. Starr, M. Laurin, S. K. Shaikhutdinov, S. Schauermann, J. Libuda, H. J. Freund, *Angew. Chem.* **2006**, *118*, 3775 – 3780; *Angew. Chem. Int. Ed.* **2006**, *45*, 3693 – 3697.
[22] H. Over, Y. D. Kim, A. P. Seitsonen, S. Wendt, E. Lundgren, M. Schmid, P. Varga, A. Morgante, G. Ertl, *Science* **2000**, *287*, 1474 – 1476.
[23] H. Over, O. Balmes, E. Lundgren, *Catal. Today* **2009**, *145*, 236.
[24] M. E. Grass, Y. Zhang, D. R. Butcher, J. Y. Park, Y. Li, H. Bluhm, K. M. Bratlie, T. Zhang, G. A. Somorjai, *Angew. Chem.* **2008**, *120*, 9025 – 9028; *Angew. Chem. Int. Ed.* **2008**, *47*, 8893 – 8896.
[25] M. E. Grass, S. H. Joo, Y. Zhang, G. A. Somorjai, *J. Phys. Chem. C* **2009**, *113*, 8616.
[26] J. Gustafson, R. Westerström, A. Mikkelsen, X. Torrelles, O. Balmes, N. Bovet, J. N. Andersen, C. J. Baddeley, E. Lundgren, *Phys. Rev. B* **2008**, *78*, 045423.
[27] J. Gustafson, R. Westerström, O. Balmes, A. Resta, R. van Rijn, X. Torrelles, C. T. Herbschleb, J. W. M. Frenken, E. Lundgren, *J. Phys. Chem. C* **2010**, *114*, 4580 – 4583.
[28] J. Gustafson, R. Westerström, A. Resta, A. Mikkelsen, J. N. Andersen, O. Balmes, X. Torrelles, M. Schmid, P. Varga, B. Hammer, G. Kresse, C. J. Baddeley, E. Lundgren, *Catal. Today* **2009**, *145*, 227.
[29] Y. Li, Q. Fu, M. Flytzani-Stephanopoulos, *Appl. Catal. B* **2000**, *27*, 181.
[30] Y. Guan, E. J. M. Hensen, *Phys. Chem. Chem. Phys.* **2009**, *11*, 9578.
[31] G. Jones, J. G. Jakobsen, S. S. Shim, J. Kleis, M. P. Andersson, J. Rossmeisl, F. Abild-Pedersen, T. Bligaard, S. Helveg, B.

Hinnemann, J. R. Rostrup-Nielsen, I. Chorkendorff, J. Sehested, J. K. Nørskov, *J. Catal.* **2008**, *259*, 150.
[32] http://www.esrf.eu/UsersAndScience/Experiments/CRG/BM26.
[33] A. Suzuki, Y. Inada, A. Yamaguchi, T. Chihara, M. Yuasa, M. Nomura, Y. Iwasawa, *Angew. Chem.* **2003**, *115*, 4943 – 4947; *Angew. Chem. Int. Ed.* **2003**, *42*, 4795 – 4799.
[34] C. H. F. Peden, D. W. Goodman, D. S. Blair, P. J. Berlowitz, G. B. Fisher, S. H. Oh, *J. Phys. Chem.* **1988**, *92*, 1563.
[35] P. A. Thiel, J. T. Yates, Jr., W. H. Weinberg, *Surf. Sci.* **1979**, *82*, 22 – 44.
[36] X. Q. Gong, Z. P. Liu, R. Raval, P. Hu, *J. Am. Chem. Soc.* **2004**, *126*, 8.
[37] Y. Zhai, D. Pierre, R. Si, W. Deng, P. Ferrin, A. U. Nilekar, G. Peng, J. A. Herron, D. C. Bell, H. Saltsburg, M. Mavrikakis, M. Flytzani-Stephanopoulos, *Science* **2010**, *329*, 1633 – 1636.
[38] Q. Fu, H. Saltsburg, M. Flytzani-Stephanopoulos, *Science* **2003**, *301*, 935 – 938.

